# The ERIS Adaptive Optics System: first on-sky results of the ongoing commissioning at the VLT-UT4

A. Riccardi*[a,d], A. Puglisi[a,d], P. Grani[a,d], R. Briguglio[a,d], S. Esposito[a,d], G. Agapito[a,d], V. Biliotti[a,d], M. Bonaglia[a,d], L. Carbonaro[a,d], M. Xompero[a,d], A. Baruffolo[b], B. Salasnich[b], G. Di Rico[c,d], R. Davies[e], H. Feuchtgruber[e], C. Rau[e], Y. Dallilar[e], K. Kravchenko[e], J. Kolb[f], P. Haguenauer[f], C. Soenke[f], D. Barr[f], A. Cortes[f], J. Reyes[f],

[a]INAF-Osservatorio Astrofisico di Arcetri, Largo E. Fermi 5, 50125 Firenze, Italy;
[b]INAF-Osservatorio Astronomico di Padova, Vicolo dell'Osservatorio, 5, 35141 Padova PD, Italy;
[c]INAF-Osservatorio Astronomico d'Abruzzo, Via Mentore Maggini, 64100 Teramo, TE, Italy;
[d]ADONI – Laboratorio Nazionale di Ottica Adattiva, Italy;
[e]Max-Planck-Institut für extraterrestrische Physik, Gießenbachstrasse 1, D-85748 Garching, Germany;
[f]European Southern Observatory, Karl-Schwarzschild-Strasse 2, D-85748 Garching, Germany

## ABSTRACT

ERIS is a new Adaptive Optics (AO) instrument installed at the Cassegrain focus of VLT-UT4 in January 2022 and led by a Consortium of Max-Planck Institut fuer Extraterrestrische Physik, UK-ATC, ETH-Zurich, NOVA-Leiden, ESO and INAF. The ERIS AO system provides NGS mode to deliver high contrast correction and LGS mode to extend high Strehl performance to large sky coverage. The AO module includes one 40x40 LGS wavefront sensor (WFS), one NGS WFS able to switching between 40x40 and 4x4 configuration, the related optics to relay the telescope beam and a dedicated SPARTA real time computer running the AO loop up to 1kHz. The AO module, with the 1170-actuator Deformable Secondary Mirror and the Laser Facility from VLT-AOF, provides AO correction to the high resolution coronagraphic imager NIX (1-5um) and the IFU spectrograph SPIFFIER (1-2.5um). In this paper we briefly review the ERIS AO system design and we present preliminary AO results of the ongoing commissioning, started in February 2022.

**Keywords:** ERIS, VLT, Wavefront Sensing, Deformable Secondary Mirror, Adaptive Optics System, SPARTA, CCD220, Laser Guide Star

## 1. INTRODUCTION

ERIS, the Enhanced Resolution Imager and Spectrograph[1], is a new 1-5 μm instrument for the Cassegrain focus of the UT4-VLT telescope that is equipped with the Adaptive Optics Facility (AOF)[2][3]. The instrument is led by a Consortium of Max-Planck Institut für Extraterrestrische Physik (MPE, leading institute), UK Astronomy Technology Centre (UK-ATC), Institute for Particle Physics and Astrophysics (ETH-Zurich), NOVA (Leiden Observatory), European Southern Observatory (ESO) and Istituto Nazionale di Astrofisica (INAF Arcetri, Abruzzo and Padova). The ERIS instrument passed the Preliminary Acceptance in Europe (PAE) in September 2020, enabling the start of the packing and shipping phase that ended with the arrival of the ERIS boxes to the VLT site (Cerro Paranal, Chile) in November 2021. The ERIS teams, in spite of the difficulties of traveling due to COVID19 pandemic, were able to move to Chile to the end of November 2021 and start the reintegration of the instrument in the New Integration Hall (NIH) at Paranal with the support of ESO. The shipping included also the DSM simulator tool[4], allowing a closed loop verification of the AO module before the installation at the telescope. The installation at the telescope was split in two runs, the first in January and the second in February 2022 (see Figure 1). At the end of the February run, ERIS had the opportunity to go on-sky receiving the first light in seeing limited on 12 Feb 2022. As soon as the following day (13 Feb) the ERIS AO team was able to close the first loop in NGS-mode (see Figure 2), proving no major issues for on-sky AO operations. In the following commissioning runs in April and June 2022, the AO related activity was focused on functionality test in order to provide a robust system in terms of setup, automated AO-aided acquisition and offsetting procedures for the various observing

*armando.riccardi@inaf.it; phone +39 055 2752 302

Adaptive Optics Systems VIII, edited by Laura Schreiber, Dirk Schmidt, Elise Vernet,
Proc. of SPIE Vol. 12185, 1218508 · © 2022 SPIE
0277-786X · doi: 10.1117/12.2629425

*Figure 1. Left: ERIS instrument in UT4-VLT dome during installation (Feb 2022). Right: ERIS installed at the Cassegrain focal station of UT4 (Feb 2022)*

modes to give reliable tools for AO operation and optimization and the parallel commissioning of the science instruments (NIX[5] and SPIFFIER[6]). An import part of the work was the on-sky testing of the interaction with the VLT-UT4 Adaptive Optics Facility (AOF) components of the Deformable Secondary Mirror (DSM[2]) and the sodium laser system (4LGSF[7]), both interfaced for the first time with ERIS only after installation on the telescope. The on-sky experiencing of the related procedures, that were set up during AIV phase, required some on-site changes in the LGS acquisition sequence and DSM operation.

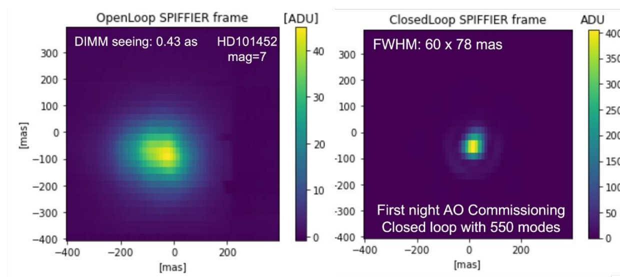


*Figure 2. Closure of the loop in the first night of AO test (13 Feb 2022)*

The run in July 2022 was mostly dedicated to Commissioning of NIX and SPIFFIER and the next run in August 2022 will be dedicated to optimization of AO performance and pushing the system toward the faint-end. Finally a run in November 2022 will be dedicated to the final tuning of ERIS observing operations in view of the Science Verification run in December 2022.

For more information on the ERIS commissioning at the full instrument level refer to Ref.[1], for the commissioning of NIX, SPIFFIER and the ERIS software refer to Ref. [5], [6] and [8], respectively.

## 2. AO LAYOUT

The AO module of ERIS is made of the following parts (see Figure 3):

- Warm-Optics (WO): an optical system relaying the telescope beam to the science instruments and the AO Wavefront Sensors (WFS). The infrared light from 1.0 to 5.5 µm is transmitted to NIX and SPIFFIER through a 45-deg $CaF_2$ dichroic that reflects the 0.4-1.0 µm light to the WFSs. The relay is made of plano or quasi-plano optics: the part with the most optical power, a telecentric lens, has 15 m focal length.
- LGS-WFS (see Figure 4-left): an on-board 40x40 Shack-Hartman (SH) WFS unit providing high-order AO correction using an on-axis Laser Guide Star (LGS). The lenslet array of the SH in imbedded in the AOF-standard WFS camera, using a 240x240 electro-multiplied (EM) CCD220 chip. The LGS WFS unit is mounted on a stage for tracking the focus of the sodium layer.
- NGS-WFS (see Figure 4-right): a second on-board SH WFS, using a Natural Guide Star (NGS) in a patrol field of $R \leq 1$ arcmin, providing 40x40 high-order correction in pure NGS-mode and 4x4 low-order (LO) correction and truth sensing in LGS-mode. The sensing is performed in the 600-1000 nm bandwidth using another EM-CCD220 camera. The NGS-WFS unit is mounted on stages to adjust focus and acquire the NGS in the patrol

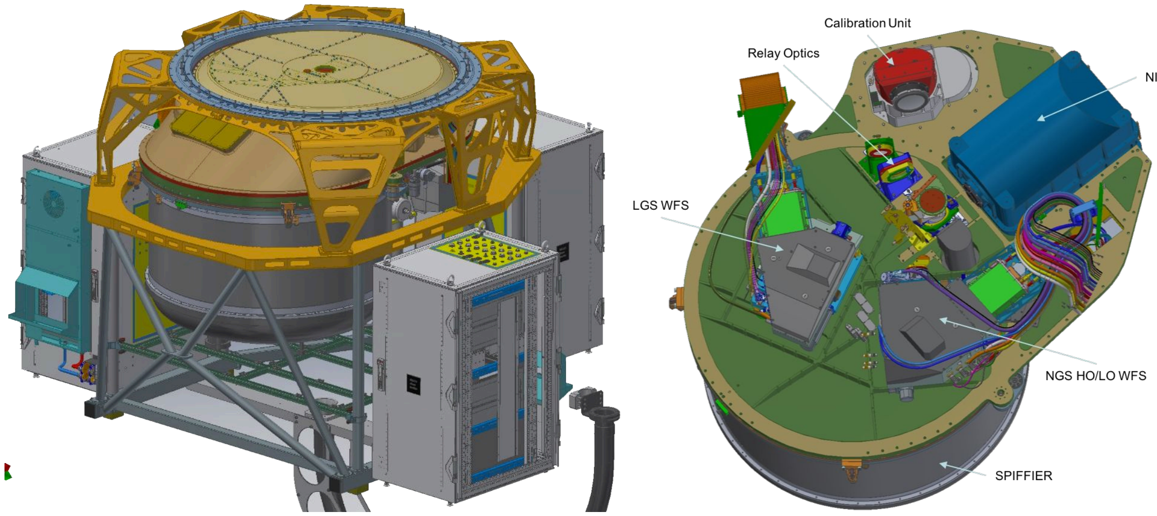


*Figure 3. Left: the ERIS instrument. Right: the ERIS sub-systems (optical bench internal view).*

field. The NGS acquisition is performed with the use of an on-board technical camera using the 400-580 nm part of the beam directed to the sensor.

- SPARTA RTC: the real-time computer (RTC), developed by ESO, located in the UT4 basement (Bodega). SPARTA interfaces the WFS cameras and commands the DSM for wavefront correction and the jitter mirror inside the LGS launcher telescope for the beacon stabilization. SPARTA provides also the real-time telemetry of the AO system. The SPARTA RTC closes the loop up to 1 kHz in NGS-mode. In LGS-mode SPARTA closes the LGS and the NGS-LO loops at 1 kHz and 500 Hz, respectively.

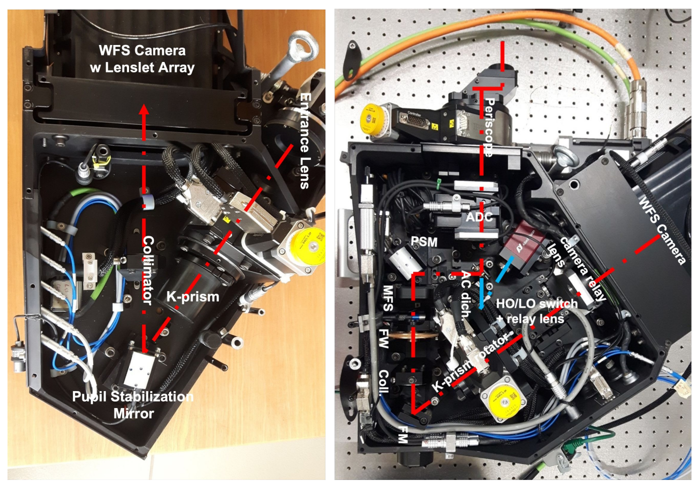


*Figure 4. WFS view after removing cover. Left: LGS-WFS Right: NGS-WFS. See Ref. [9] for a detailed description of the components.*

For a more detailed description of the ERIS AO module and its components, refer to Ref. [9].

## 3. AO CONTROL

The AO control scheme in LGS-mode is shown in Figure 5, reporting both the Real Time (RT) and Auxiliary loops. The NGS-mode scheme is obtained by the same graph with the LGS-related parts deactivated.

The LO and LGS tip-tilt (TT) loops and the Truth Sensing are closed using a Control Matrix (CM) calibrated on-sky, while the NGS and LGS HO loops are closed with a Pseudo-Synthetic CMs. The process of generating the HO pseudo-synthetic CMs is the following:

1. The DSM set of commands defining the Karhunen-Loève (KL) basis is computed by diagonalizing the Von-Karman-filtered covariance matrix of the influence functions (IFs) generated by Finite Element Analysis (FEA). The FEA IFs are pre-processed to slave the non-working and unseen actuators[10]. Unseen actuators are currently the ones in the inner ring and the ones shadowed by the retracted M3. The first three modes (Tip, Tilt and Focus) are forced to be pure Zernike modes. The KL modes are orthogonal over the actual ERIS pupil. See Figure 6 for

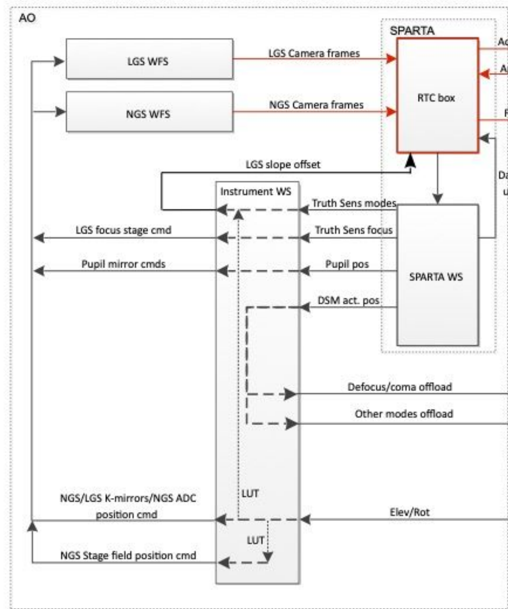


*Figure 5. LGS-mode AO Control scheme. NGS-mode scheme is obtained disabling the LGS-related components.*

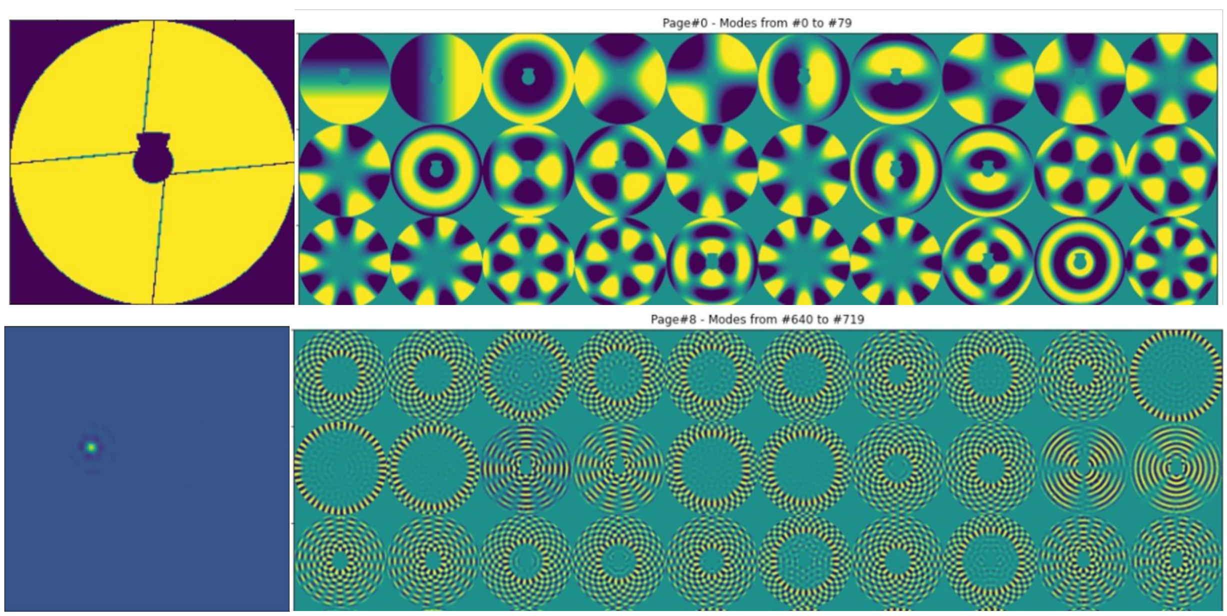


*Figure 6. Top-left: pupil seen by ERIS. the asymmetry of the central obscuration is due to the M3 shadow in retracted position. Bottom-left: Example of Influence Function used to generate Karhunen-Loève basis. Right: subset of generated KL modes.*

the generated KL basis. The process produces the M2C matrix, transforming the KL modal coefficients to DSM actuator commands.

2. A zonal Interaction Matrix (IM) is calibrated on-sky using an Hadamard actuation scheme[11] to increase SNR and obtain a measurement in a few seconds on a bright star.
3. The parameters defining the projection of the DSM FEA IFs over the SH sub-apertures geometry (i.e. the pupil registration) are obtained by fitting the Pseudo-Synthetic IM (PSIM, computed with the projected FEA IFs) to

the on-sky calibrated IM. The fitting method is the same implemented for the AOF [12]. See Figure 7 for a comparison between the on-sky calibrated IM and the fitted PSIM.

4. The CM is computed by filtering the first $n$ KLs as follows:
   $CM_n = M2C_n \cdot diag(g_n) \cdot (PSIM \cdot M2C_n)^+$, where $^+$ is the pseudo-inverse operation and $g_n$ is the vector of the modal integral gains of the first $n$ KL modes.

Even if the SPARTA output is zonal (DSM actuator commands), the use of the $g_n$ vector provides an effective modal filtering (pure integrator) of the AO correction, allowing the optimization of the modal gains at the cost of reloading the full CM. The optimization algorithm used in ERIS is a z-transform implementation of the standard one from Gendron & Léna[13] with optimal gain computed in modal slots to increase the SNR. Figure 8 shows the on-sky verification of the optimization process.

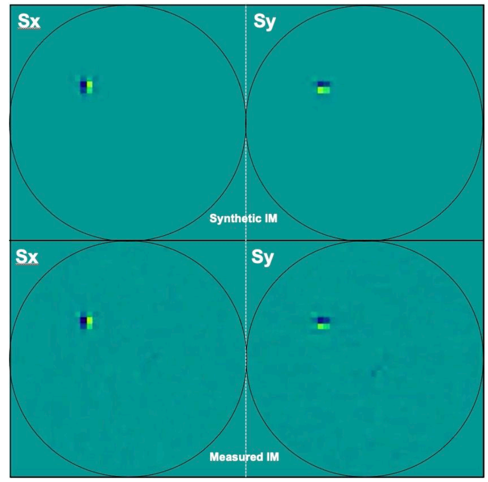


*Figure 7. Comparison of WFS signals generated by pushing a single actuator for the measured Interaction matrix (bottom) and a Pseudo-Synthetic IM (top). Note the background noise in the measured IM.*

To stabilize the pupil centering on the LGS/NGS 40x40 SH grid, a pupil loop is closed commanding the on-board pupil stabilization mirror. The feedback is provided by the fitting of the geometrical transform and apodization pattern of the pupil shape in Figure 4 over the averaged intensity pattern of the SH sub-apertures.

## 4. VERIFICATION OF CLOSED LOOP PERFORMANCE IN BRIGHT-END REGIME

Figure 9 shows a typical comparison between Closed-Loop (CL) and Open-Loop (OL) PSF in the bright-end regime of the NGS-mode at the Brγ (λ=2170 nm) wavelength. The diffraction rings are well visible and regular, confirming a negligible effect of the NGS-mode Non-Common-Path Aberrations (NCPA), currently not compensated. In fact, during the AIV phase, the NCPA have been calibrated in closed loop with the DSM simulator for both NIX and SPIFFIER, showing a contribution ranging from 22 to 32 nm rms WFE depending on the instrument camera+filter(s) configuration (30 nm in the configuration of Figure 9). The really small amount of NCPA is mostly due to the design choice of using stages for NGS acquisition instead of a Field Steering Mirror (FSM). The need of no FSM, together with the need of no Deformable Mirror (DM) on-board of ERIS, allowed the usage of quasi-plano optics for the telescope beam relay (WO) to keep under control NCPA.

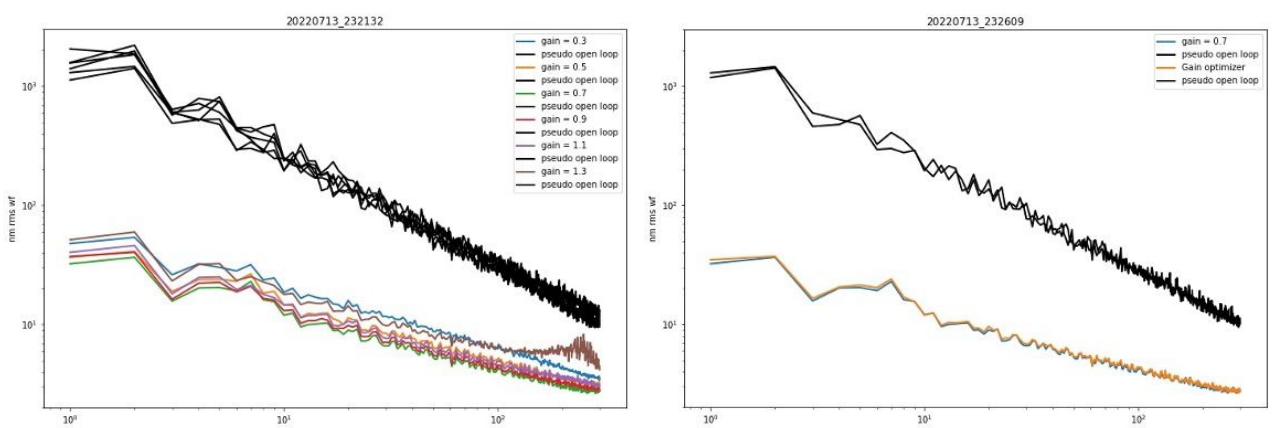


*Figure 8. RMS of modal coefficient of correction residuals vs modal index (tip, tilt, focus, etc.) in NGS-mode. Left: modal residuals plots as a function of loop integral gain (equal gain for all the modes). The curve reaches a minimum residual at gain 0.7. Right: superimposition of the 0.7-gain curve and the curve obtained after running the modal gain optimizer process, the optimizer converged to the minimum residual curve. The process optimize the gain for modes in ranges. Tip, tilt and focus are always singularly optimized, The higher order modes are grouped in sets of complete radial orders.*

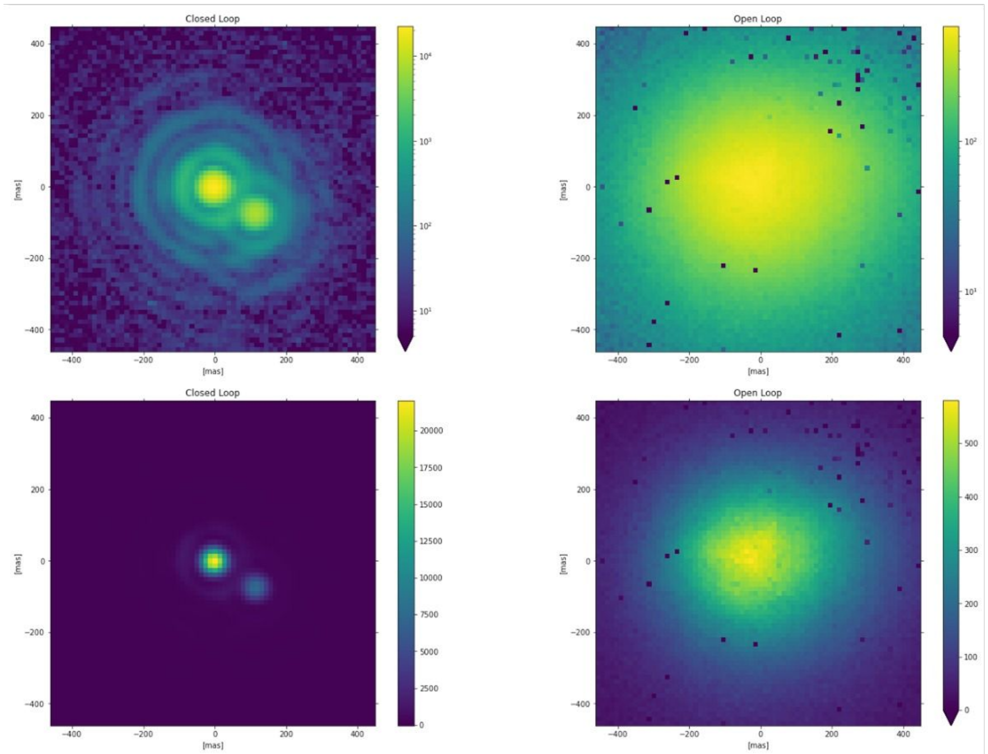


*Figure 9. Example of NGS-mode closed (left) and open loop (right) PSF: double star 17369-1757HDS2486, mag($G_{RP}$)=8.6. Top: log-scale PSF. Bottom: linear scale PSF.*

The AO requirements in the bright-end NGS- and LGS-modes specify:

- NGS-mode: 68% in Ks band ($\lambda_c$=2160 nm) with mag = 8 and seeing$_{LoS}$ = 0.87 arcsrc along the Line of Sight;
- LGS-mode: 54% in Ks band with mag=12 and seeing$_{LoS}$ = 0.87 arcsec.

The achieved SR values are (see Figure 10 and Figure 11):

- NGS-mode: 80% in Brγ ($\lambda$=2170 nm) filter with mag = 7.8 and seeing$_{LoS}$ = 0.82 arcsec (no NCPA compensation);
- LGS-mode: 61% in Brγ filter with seeing$_{LoS}$ = 0.57 arcsec (no Truth Sensing activated, except for the focus term).

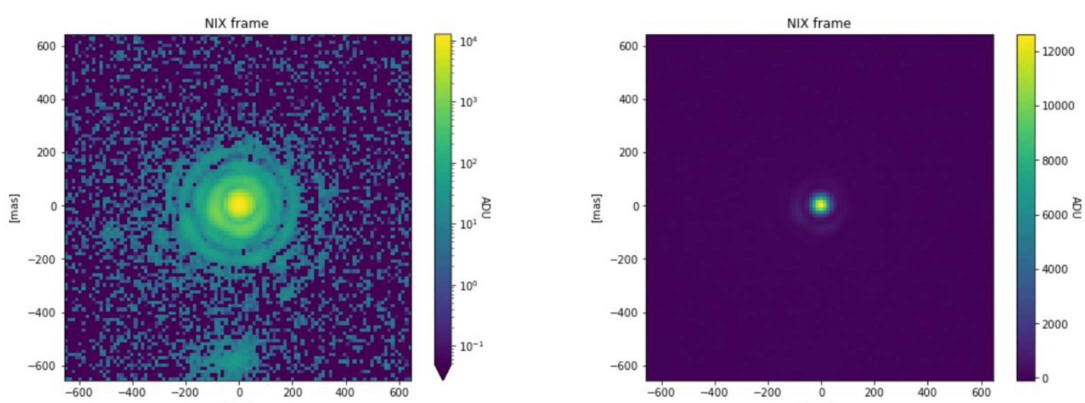


*Figure 10. Bright-end PSF in NGS-mode: SR=68% at 2170 nm, FWHM=53 mas (Moffat fit). Seeing was 0.82 arcsec. No NCPA compensation.*

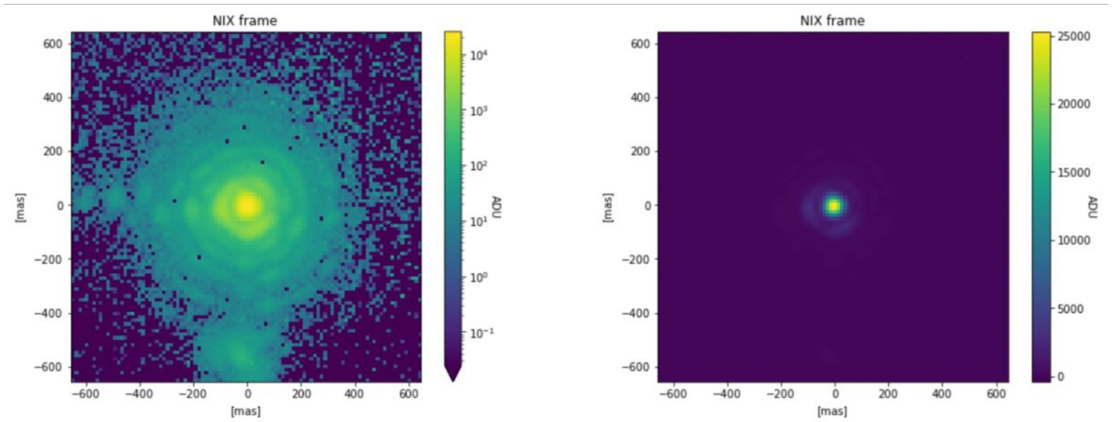


*Figure 11. Bright-end PSF in LGS-mode: SR=61% at 2170 nm, FWHM=53 mas (Moffat fit). Seeing was 0.57 arcsec. Truth Sensing only for focus term.*

Figure 12 shows the comparison among the achieved bright-end performance, the corresponding requirements and the results of simulations from the design phase[9]. In NGS-mode it is clear that the performance is in good matching with the simulations and largely satisfying the requirements. In LGS-mode the seeing of the measurement was better than specified, however the result shows there are not major issues in reaching the bright-end requirement.

Part of the next commissioning run will be dedicated to push the performance in the faint-end in both NGS- and LGS-mode, and characterize the Truth Sensing in the LGS-mode.

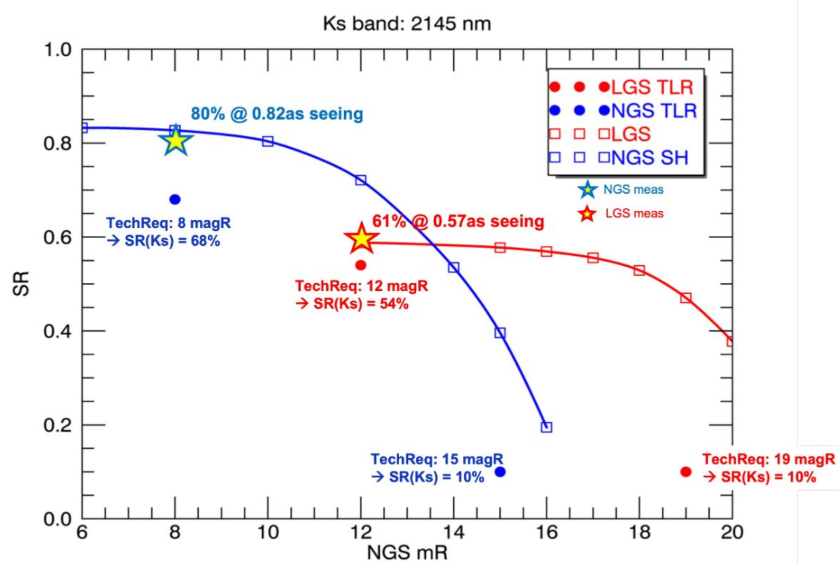


*Figure 12. SR(Ks) vs NGS magnitude. Comparison among measured points (stars), Requirement specifications (filled circles) and design phase simulations (lines).*

## 5. CONCLUSIONS

The ERIS instrument has been installed at the Cassegrain focal station of UT4-VLT and opened to the sky in Feb 2022, providing the first successful closed-loop operation right on the first day dedicated to the on-sky AO test (13 Feb 2022). The AO is currently in the commissioning phase, showing good performance in the bright-end (NGS-mode SR(2170nm)=68%; LGS-mode SR(2170nm)=61%). The functionality of the AO system in interaction with the science instruments is quite robust, both in terms of acquisition procedure in all the observing modes and supporting the various types of AO-aided offsets that are requested for observations.

The next commissioning runs will be dedicated to push the performance in the faint-end in both NGS- and LGS-mode (Aug 2022), and consolidate the experience of AO-aided observations in a more extended range of operating conditions (Nov 2022). Science Verification of ERIS is currently scheduled in Dec 2022 and the release to the observing community starting from Apr 2023.

## 6. ACKNOWLEDGMENTS

The ERIS AO team thanks the ESO staff in Paranal for the great support, the problem-solving attitude and the enthusiasm for the project.

## REFERENCES

[1] Davies, R., *et al.* "ERIS first light results," Proc SPIE 12185 (2022).
[2] Madec, P.-Y., *et al.* "Adaptive Optics Facility: from an amazing present to a brilliant future," Proc. SPIE 10703, 1070302 (2018).
[3] Oberti, S., *et al.* "The AO in AOF," Proc. SPIE 10703, p. 107031G (2018).
[4] Briguglio, R., *et al.* "The simulator of the VLT Deformable Secondary Mirror: a test tool for adaptive optics instruments for the Yepun-UT4 telescope," Proc. SPIE 12185 (2022)
[5] Yigit, D., *et al.* "First on-sky results with the infrared imager ERIS/NIX at VLT," Proc. SPIE 12184 (2022).
[6] Kravchenko, K., *et al.* "The on-sky performance of the IFU spectrograph ERIS/SPIFFIER during its commissioning phase," Proc SPIE 12184 (2022).
[7] Hackenberg, W. K., *et al.* "ESO 4LGSF: Integration in the VLT, Commissioning and on-sky results," Proc SPIE 9909 (2016).
[8] Baruffolo, A., *et al.* "Commissioning of ERIS Instrument Software," Proc. SPIE 12189 (2022).
[9] Riccardi, A., *et al.* "The ERIS adaptive optics system: from design to hardware," Proc SPIE 10703, p. 1070303 (2018).
[10] Riccardi, A. "Slaving and disabling actuators with voice-coil adaptive mirrors," INAF Technical Reports n. 68 (2020) http://hdl.handle.net/20.500.12386/29767
[11] Kasper, M. *et al.* "Fast calibration of high-order adaptive optics systems," JOSAA 21, pp. 1004-1008 (2004)
[12] Kolb, J., *et al.* "Calibration strategy of the AOF," Proc. SPIE 8447, p. 85 (2012)
[13] Gendron, E., Léna, P. "Astronomical adaptive optics I. Modal control optimization" A&A 291, pp 337-347 (1994)